Near Sea-Surface Mobile Radiowave Propagation at 5 GHz: Measurements and Modeling

Yee Hui LEE[1], Feng DONG[1], Yu Song MENG[2]

[1]School of Electrical and Electronic Engineering, Nanyang Technological University,
50 Nanyang Avenue, Singapore 639798, Singapore
[2] National Metrology Centre, Agency for Science, Technology and Research (A*STAR)
1 Science Park Drive, Singapore 118221, Singapore

eyhlee@ntu.edu.sg, ysmeng@ieee.org, meng_yusong@nmc.a-star.edu.sg

Abstract. *Near sea-surface line-of-sight (LoS) radiowave propagation at 5 GHz was investigated through narrowband measurements in this paper. Results of the received signal strength with a transmission distance of up to 10 km were examined against free space loss model and 2-ray path loss model. The experimental results have good agreement with the predicted values using the 2-ray model. However, the prediction ability of 2-ray model becomes poor when the propagation distance increases. Our results and analysis show that an evaporation duct layer exists and therefore, a 3-ray path loss model, taking into consideration both the reflection from sea surface and the refraction caused by evaporation duct could predict well the trend of LoS signal strength variations at relatively large propagation distances in a tropical maritime environment.*

Keywords

Evaporation duct, maritime mobile, modeling, path loss prediction, sea reflection.

1. Introduction

Radiowave propagation in maritime environments has been of great interest to many researchers over the years [1–9]. The understanding of over-sea radiowave propagation is very important for system designers when planning to establish a reliable radio link between a sea vessel and an on-shore base station (BS). Over the years, different application scenarios have been investigated; in [2–4], over-the-horizon fixed links were examined; in [6], [7], mobile channels were studied; and in [8], [9], slant-path propagation for aeronautical applications was analyzed.

Recently, there has been growing interest in implementations of wireless systems in 5 GHz band for maritime environments, mainly in the applications of WiMAX at seaports [10] and for military off-shore anti-terrorist surveillance [11]. These applications require the 5 GHz systems to be operated in a near sea-surface line-of-sight (LoS) mobile environment (e.g., between a BS and a moving vessel). The radio channel for this scenario differs from those reported in [1–4], [8], [9]. Moreover, our previous investigations [9], [12] indicate that ducting is significant for radiowave propagation over the tropical ocean of Singapore in 5 GHz band. Therefore, although similar scenarios [5–7], [13] were reported, their maritime conditions and frequencies are different and may not be applicable to the 5 GHz radio link over a tropical ocean where the occurrence of an evaporation duct is known to be of a higher probability and more predominant [5].

From the literature, it is well-recognized that radiowave propagation over a sea surface is affected by the ducts such as surface ducts, elevated ducts, and evaporation ducts [14], [15]. For near sea-surface LoS propagation, the effects of evaporation duct are obvious and dominant amongst all the ducts. This is because the evaporation duct exists over the ocean almost all of the time [14], since it is a result of the rapid decrease in vapor pressure from a saturation condition at the sea surface to an ambient vapor pressure at levels several tens of meters above the sea surface. This decrease in vapor pressure generally results in a decrease in the modified refractivity and thus, creates a ducting layer adjacent to the sea surface. Research work in [2] indicated that an evaporation duct above the sea surface can result in a substantial increase in the received signal strength at frequencies above 3 GHz. Measurement results in [3] also showed an enhancement in signal strength of more than 10 dB, observed 48% of the time along a 27.7 km over-sea path at 5.6 GHz.

Therefore, it is important to study the effect of evaporation duct in characterizing and modeling of near sea-surface radiowave propagation at the frequency of 5 GHz. As a continuation of our previous work [16] where channel characteristics of a non-line-of-sight (NLoS) sea-surface link at 5 GHz for Singapore maritime environment was reported, the main objective of this paper is to perform a detailed investigation on near sea-surface LoS propagation through path loss modeling with the considerations the evaporation duct and the sea-surface reflection.

In the following, measurement campaign is described in Section 2. In Section 3, free space loss model and 2-ray path loss model are examined against the experimental results first. Based on the observed discrepancy, a 3-ray path loss model is introduced to take into consideration the refracted wave by evaporation duct. Section 4 then gives a discussion on empirical estimations of the effective duct height. Finally, conclusions of this paper are given in Section 5.

(a) Transmitter on a speed boat

(b) Receiver on shore

Fig. 1. Setup of transmission and data-logging systems for near sea-surface LoS measurements.

2. Measurement Campaign

2.1 Measurement System

Fig. 1 shows the main equipment and setup used for narrowband measurements. It is noted that 5.15 GHz was chosen and approved for continuous-wave transmission where no interfering signal was detected. As shown in Fig. 1a, an omni-directional antenna was mounted on top of a speed boat at a height of approximately 3.5 m above sea level. It was connected to a signal generator and a high-power amplifier housed within the boat cabin, forming a mobile transmitter with an output power of 30 dBm. During the measurements, GPS data was continuously logged so as to obtain the instantaneous time, altitude, longitude and latitude coordinates. The pitch and roll of the moving boat was logged using a fluxgate compass.

The BS was on shore, close to the sea. In order to ensure a LoS condition between the transmitter and the receiver, the receiver consisted of an identical omni-directional antenna installed on the roof of a building as shown in Fig. 1b with different heights above sea level (in order to study the effect of antenna height), and connected to a spectrum analyzer. The span of the spectrum analyzer was set to 20 kHz around its center frequency to reduce the noise bandwidth. Peak marker readings of the received signal were recorded at intervals of 1 second using a Labview program. All the data recorded was time-stamped for synchronization with the location, heading and orientation of the mobile transmitter.

The whole system was carefully calibrated on-site before the sea trials, and checked again after the measurements. The system effect was minimized through the removal of the antenna gains and the measurement of a back-to-back connection between the transmitter and the receiver. Weather conditions were also recorded using a weather meter at the transmitter side and a weather station at the receiver side respectively. However due to the lack of more suitable meteorological instruments such as a weather balloon, the weather information was restricted at the transmitter and receiver altitude levels.

Fig. 2. Measurement route and receiver location, taken from Google Earth.

Parameter	Value
Carrier frequency	5.15 GHz
Transmitted power	30 dBm
Transmitter height	3 to 4 m
Receiver height	20 m, 10 m and 7.6 m
Maximum route distance	10 km
Antennas type	Omni-directional

Tab. 1. Summary of measurement parameters.

2.2 Measurement Routes

Measurements were carried out over an open sea area off the southeast coast of Singapore. BS was located at a yacht club (N $01°19'09''$, E $104°1'22''$). The mobile transmitter was on board a speed boat with a maximum speed of 30 knots. During the trials, the boat traveled along a 10 km route as shown in Fig. 2 with a speed of approximately 6 knots. LoS was maintained throughout the measurements except for some occasional passing-by ships for a short period of time. For each receiver height, multiple trials on different days have been carried out in order to compare and

verify the results. It is noted that all the measurement campaign was conducted under similar sea status; calm or near calm. The main measurement parameters are summarized in Tab. 1.

3. Near Sea-Surface Path Loss Model

ITU-R P.1546 model [13] provides a set of curves for prediction of propagation loss over a sea path at a frequency from 30 MHz to 3 GHz, which limits its application in our study at 5.15 GHz. However, a general trend can be observed from those field strength versus distance curves in [13] that radiowave propagation over sea paths (path distance less than 10 km) approaches free space propagation at 50% of time when the frequency increases. Since the frequency of operation in this study is 5.15 GHz, free space loss (FSL) model could therefore be used. Moreover, works in [5] also reveals that propagation loss of a 5-GHz over sea-water radio link can be predicted using the FSL model when the transmission range is less than 10 nautical miles (18.52 km) but with some interference nulls.

These nulls could be due to the interference between the direct ray and the sea-surface reflected ray. Our previous study [9] also found that around 86% of all the trials for over-sea radiowave propagation can be represented by a 2-ray multipath model (i.e., a direct ray with a sea-surface reflected ray) over the tropical ocean. Although the information in [9] is for aeronautical applications, there is a very high probability for the existence of a sea-surface reflected wave for near sea-surface LoS propagation. Therefore in this section, we will examine the received signal strength against the predicted results using the FSL model and the 2-ray path loss model.

3.1 Propagation Loss Models

For the radiowave propagation in free space, the propagation loss can be predicted by the FSL model [17],

$$L_{FSL} = -27.56 + 20\log_{10}(f) + 20\log_{10}(d) \qquad (1)$$

where L_{FSL} is the free space loss in dB, f is the frequency in MHz, and d is the propagation distance in meters.

When a reflected ray from the sea surface exists besides the LoS path (direct ray), the propagation loss could be predicted by a 2-ray path loss model. Since there is a near-grazing incidence on the sea surface in our measurements, the reflection coefficient for a vertically polarized wave approaches -1. Therefore, the 2-ray path loss model can be simplified as [17]

$$L_{2-ray} = -10\log_{10}\left\{ \left(\frac{\lambda}{4\pi d}\right)^2 \left[2\sin\left(\frac{2\pi h_t h_r}{\lambda d}\right)\right]^2 \right\} \quad (2)$$

where L_{2-ray} is the 2-ray propagation loss in dB, λ is the wavelength in meters, and h_t, h_r are the heights of a transmitter and a receiver in meters. In the following, both the
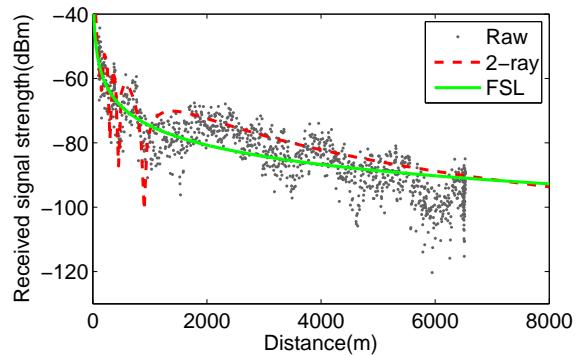
FSL model and the 2-ray model will be used to predict the received signal strength under ideal conditions for near sea-surface radiowave propagation at 5.15 GHz.
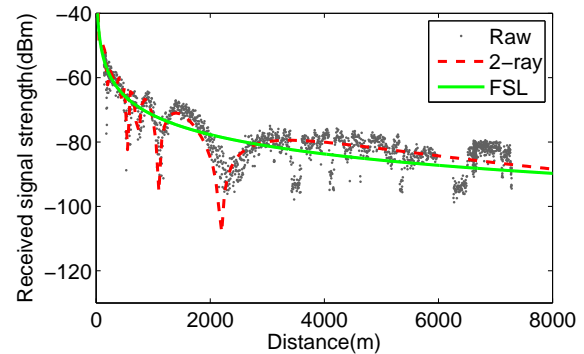
(a) Results at h_r = 20 m conducted on 23 November 2011
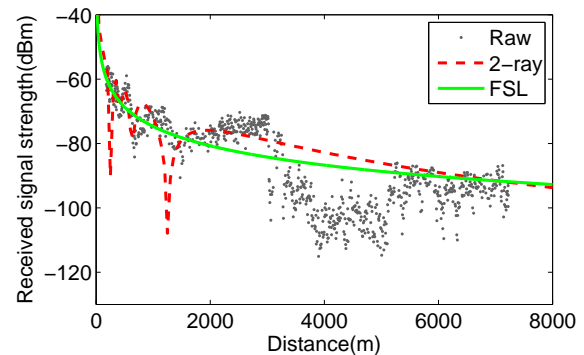
(b) Results at h_r = 10 m conducted on 28 September 2011

(c) Results at h_r = 7.6 m conducted on 3 April 2012

Fig. 3. Received signal strengths versus distance at different receiver heights; measured and predicted.

3.2 Comparison with the Predicted Results

Typical measurement results at the receiver height h_r of 7.6 m, 10 m, and 20 m are shown in Fig. 3, together with the predicted signal strengths using the FSL model and the 2-ray model (assuming a perfect sea-surface reflection). From Fig. 3, it can be observed that the FSL model is able to predict the exponential decreasing strength trend for all the 3 receiver heights. The FSL model is well-suited for prediction of the local mean (large scale) propagation loss. These observations are consistent with those reported in [5], [13]. More interestingly, when the propagation distance is less than about 2000 m to 3000 m (from Fig. 3), the measured

results show a similar trend as the predicted results using the 2-ray model for all the measurement scenarios. That is, there are some interference nulls which are due to the destructive summation of the radiowaves (the direct wave and the sea-surface reflected wave from modeling process of the 2-ray model) arriving at the receiver. The slight misalignments of the predicted nulls with respect to the measured ones in Fig. 3 are due to the sea-surface roughness [18], [19] and the refraction of the propagating waves mainly. Both of them can weaken the applicability of 2-ray path loss model which is assumed for a perfect reflection and straight rays.

However, it is observed from Fig. 3 that as the propagation distance increases beyond about 2000 m to 3000 m (known hereby as the break point d_{break}), the prediction abilities of both the FSL model and the 2-ray model become poor for near sea-surface LoS environments. There are some interference nulls beyond d_{break} that cannot be predicted using both the models. As seen in Fig. 3, both the models tend to approach a stable signal level with an exponential decay.
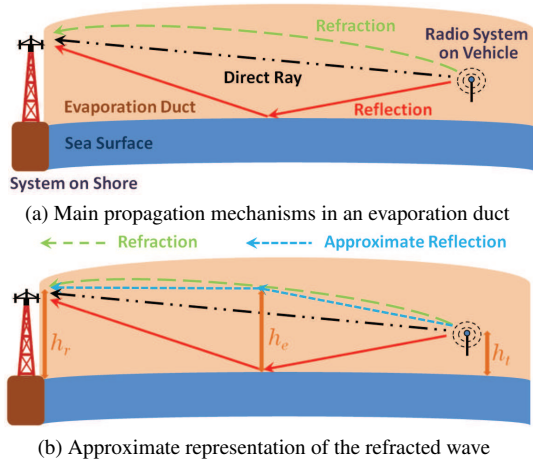

(a) Main propagation mechanisms in an evaporation duct

(b) Approximate representation of the refracted wave

Fig. 4. Near sea-surface radiowave propagation where a refracted wave is approximately represented as a reflected wave.

These additional interference nulls beyond d_{break} could be due to an additional ray which appears as the propagation distance increases. It can be a refracted ray (as shown in Fig. 4) caused by the evaporation duct which exists over the tropical sea surface almost all of the time [14]. From the reported works, the evaporation duct can trap the over-water propagating signals [20]. Therefore, a multi-ray path loss model which takes into consideration the signals trapped in an evaporation duct should be considered beyond d_{break}.

In order to estimate this break point d_{break}, we reviewed the trends of the FSL model and the 2-ray model. As the distance increases beyond the last null predicted by 2-ray model, both the models tend to level out slowly. Therefore, it could be concluded that the 2-ray path loss model will provide accurate predictions roughly up to a distance of its last predictable null (or more precisely the first maximum after the last predictable null). This break distance d_{break} can be roughly estimated as

$$d_{break} = \frac{4h_t h_r}{\lambda}. \tag{3}$$

In our measurement campaign, d_{break} is around 4000 m, 2000 m and 1500 m when h_r is 20 m, 10 m and 7.6 m respectively. For path loss modeling beyond d_{break}, a multi-ray path loss model is considered. In the following, a 3-ray path loss model, taking into consideration the refraction due to the evaporation duct as shown in Fig. 4 is proposed.

3.3 Modeling with the Ducting Effect

As discussed above, 2-ray path loss model will lose its prediction ability when the propagation distance exceeds d_{break} roughly. For example, interference nulls observed in Fig. 3a at around 900 m, 1100 m and 2100 m ($< d_{break}$, $d_{break} \approx 4000$ m) can be predicted using the 2-ray model. While the nulls at 4100 m, 5300 m and 6200 m ($> d_{break}$) cannot be predicted by the 2-ray model. The interference nulls could be caused by the trapped wave within the evaporation duct as illustrated in Fig. 4.

Although a distance of about 5000 m is reported as the one after which the ducting should be accounted for in [21], there is a higher probability for a shorter ducting distance (e.g., < 4500 m) in the tropical ocean where our measurements were carried out. This is because the evaporation duct heights in tropical waters are typically larger than those reported for temperate cooler waters [22]. It therefore could start to trap the radiowaves at a shorter distance. The trapped wave in the evaporation duct is more likely due to the radiowave refraction as shown in Fig. 4a. This is because the upper boundary of the evaporation duct layer is not homogenous [20], the radiowaves incident onto the upper boundary would be diffused immediately and make the reflection from the boundary insignificantly in the received field. Moreover for the refraction, the refracted ray (3rd ray) will not appear at short distances, but would appear as the distance increases. Especially when the distance increases much further, more additional rays could also appear although there is minor probability for them to happen in our measurements.

Therefore in this study, a 3-ray path loss model (including a direct LoS ray, a reflected ray from sea surface, and also a refracted ray by evaporation duct) is used for modeling and predicting near sea-surface LoS propagation preliminarily. Although there are other methods which may be better for modeling the radiowave propagation in a duct (e.g., parabolic equation approximation method [19]), ray-tracing is preferred in this study due to the simplicity of its final mathematical expression that describes the scenario and hence, its straightforward application in radio planning. As shown in Fig. 4b, the refracted ray is approximately represented by a near-grazing reflected wave to simplify the process of ray-tracing modeling since the antenna heights are much smaller than the propagation distance.

For 3-ray path loss modeling, the evaporation duct layer is assumed to be horizontally homogeneous. Similar to

the 2-ray path loss model described earlier, a near-grazing incidence on the sea surface is assumed and finally, the reflection coefficient for a vertically polarized wave approaches to -1. With these assumptions, the 3-ray path loss model [23] can be simplified into (4),

$$L_{3-ray} = -10\log_{10}\left\{ \left(\frac{\lambda}{4\pi d} \right)^2 [2(1+\Delta)]^2 \right\}, \quad (4)$$

with

$$\Delta = 2\sin\left(\frac{2\pi h_t h_r}{\lambda d} \right) \sin\left(\frac{2\pi(h_e - h_t)(h_e - h_r)}{\lambda d} \right) \quad (5)$$

where h_t and h_r are the heights of the transmitter and the receiver in meters, and h_e is the effective duct height as shown in Fig. 4b. h_e is approximately equal to (or slightly less than) the height of evaporation duct layer which is used as a reference in 3-ray path loss modeling. A preliminary investigation of 3-ray path loss modeling is then performed through evaluating the measured signal strengths against the estimated ones using (4) with different h_e assumed. Fig. 5 shows an example of results with $h_e = 25$ m and 35 m respectively.
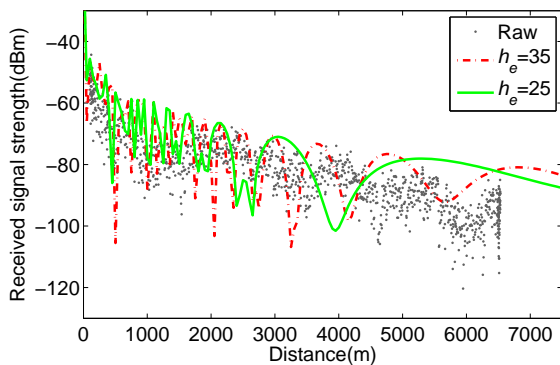

Fig. 5. Example of the received signal strength versus distance with the estimated values using 3-ray model with $h_e =$ 25 m and 35 m.

From Fig. 5, it can be observed that the signal nulls beyond d_{break} of 1500 m in the measured results which cannot be predicted by the 2-ray model previously could be estimated using the 3-ray model. The misalignments of the measured nulls with the predicted ones are due to the improper values assigned to h_e. Therefore for modeling of radiowave propagation over a tropical sea surface, 3-ray path loss model that not only considers the direct ray and the sea-surface reflected ray, but also the refracted ray by an evaporation duct, should be considered.

4. Estimation of Effective Duct Height

In order to know the effective duct height h_e as shown in Fig. 4b, the height h of a typical evaporation duct which is approximately equal to (or slightly higher than) h_e is used as a reference. For deriving h, weather information such as humidity, temperature, wind speed and pressure is required at

regular vertical intervals above the sea surface up to a height of 40 m or more. However, due to the limitation of meteorological instruments (e.g., lack of a weather balloon as we mentioned above), it is difficult to get the vertical weather information on site which restricts an accurate estimation of h. Therefore, the single point weather information collected at both the transmitter and receiver has to be used to estimate the duct height h for all the 21 measurement campaign, using a modified P-J formulation given in [24]. The P-J formulation was developed for an open ocean and therefore it may lose the prediction accuracy when applied to this coastal environment. It is also noted that the P-J formulation is very sensitive to the weather information.
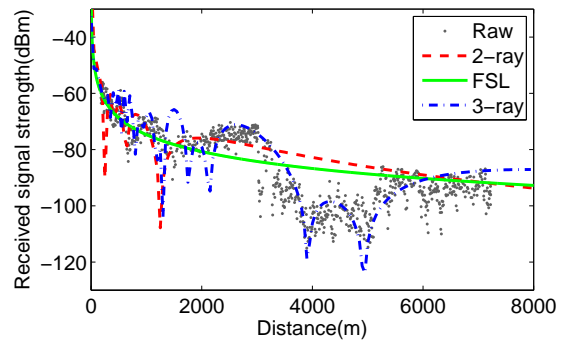

Fig. 6. The received signal strength versus distance with the predicted results using the FSL, 2-ray and 3-ray models: an example with $h_r = 10$ m.

An empirical method of determining the effective duct height h_e is therefore performed through the curve fitting/regression technique on the measured data in this study. The method is similar to the one reported in [25] where h_e was obtained based on a split-step Fourier solution of the parabolic equation approximation to the wave equation. Empirical values of h_e in (5) are then estimated by performing curve fitting onto our measurement data to align the predicted nulls with the measured ones at larger distances for each trial. An example of the curve fitting of 3-ray path loss model to the experimental results for determining h_e is shown in Fig. 6. For completeness, both the FSL model and the 2-ray model are also shown in Fig. 6.

From Fig. 6, it can be observed that the fitted 3-ray model shows a good prediction ability when the propagation distance is beyond d_{break}, especially for the sudden drop of the received signal level at distances between 4 km and 5 km. The sudden signal drop is due to the destructive summation of additional refracted wave by evaporation duct with the LoS ray and the sea-surface reflected wave. The effective evaporation duct height h_e obtained from the curve fittings of (4) to the measurement data is able to predict the signal variations very well. The observations hold for all the 21 measurement campaign performed over the tropical sea environment, and correspondingly h_e are estimated and summarized in Fig. 7 with the calculated h using the P-J formulation [24].

The observations from Fig. 6 also indicate that the 3-ray path loss model taking into consideration the contribu-

tion of the refracted wave by evaporation duct is more appropriate for near sea-surface propagation loss prediction as compared to the popular 2-ray path loss model particularly at a distance beyond d_{break}. This is because the ducting effect usually becomes significant for long-range over-sea radiowave propagation. When the propagation distance is below d_{break}, the ducting effect is almost negligible where the reflection from the sea surface and the direct LoS ray dominate. Thus, the 2-ray model should be only used for short-range ($< d_{break}$) near sea-surface propagation.

Moreover from the literature, it is found that the occurrence probability of an evaporation duct around nearby marine environments such as the South China Sea is around 80%, and the annual average height h of the evaporation duct is around 7 m to 15 m [26]. These values are similar to those calculated h using the P-J formulation as shown in Fig. 7a.
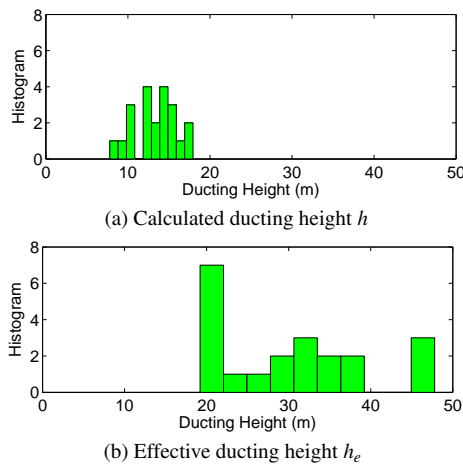

(a) Calculated ducting height h

(b) Effective ducting height h_e

Fig. 7. Histograms of the calculated duct height h and the empirical estimated effective duct height h_e.

However, the results in Fig. 7b show that most (around 86%) of the estimated h_e (supposed to be approximately equal to/slightly less than h) in this study falls within the range of 20 m to 40 m, with a median value of 30.5 m. This statistic is found to be close to those reported in [26] where the averaged evaporation duct height h at nearby marine environment is between 25 m to 40 m during similar months of March, April, September and November. Another example for the empirical h at a similar environment is reported in [22], which was based on the data measured between the Palm Islands and the Australian mainland in Northern Queensland which is also with a tropical climate. The duct height h is found to increase as the wind speed increases, and can be up to 25 m at a wind speed of 10 knots roughly. Referring to the reported information in [22], the estimated effective duct height h_e in Fig. 7b which has a measured wind speed within the range of 10 knots to 15 knots looks reasonable.

The values of h_e in Fig. 7b are then more reliable than the calculated h using the P-J formulation which mainly falls into the range of 8 m to 18 m as shown in Fig. 7a. That is, the P-J formulation tends to underestimate the actual duct

height in this coastal environment. A possible reason for this observed discrepancy may be because: the measurements were made in a coastal environment where stable atmospheric conditions could exist, while the P-J formulation is for an open ocean which may lead to underestimation of the evaporation duct height as discussed [4].

5. Conclusions

This paper reported an experimental investigation of near sea-surface LoS radiowave propagation at 5 GHz through narrowband measurements. Good agreement has been observed between the measured results and the predicted values using a 2-ray path loss model when the propagation distance is less than d_{break}. However when the propagation distance increases beyond d_{break}, its prediction ability becomes poor.

Our results and analysis indicated that a 3-ray path loss model taking into consideration the refracted wave by an evaporation duct and the reflection from the sea surface could well predict the trend of the signal strength variations in the tropical marine environments when the propagation distance increases beyond d_{break}. The results also show that most (around 86%) of the estimated effective duct height h_e falls into the range of 20 m to 40 m with a median value of 30.5 m, which is close to the reported average height h of evaporation duct at a nearby marine environment.

Therefore for radio planning, near sea-surface LoS radiowave propagation loss L in dB could be estimated generally with the following,

$$
L = \begin{cases} -10\log_{10}\left\{\left(\frac{\lambda}{4\pi d}\right)^2 \left[2\sin\left(\frac{2\pi h_t h_r}{\lambda d}\right)\right]^2\right\}, & d \leq d_{break}, \\ -10\log_{10}\left\{\left(\frac{\lambda}{4\pi d}\right)^2 \left[2\left(1+\Delta\right)\right]^2\right\}, & d > d_{break}. \end{cases}
$$

Here, $\Delta = 2\sin\left(\frac{2\pi h_t h_r}{\lambda d}\right)\sin\left(\frac{2\pi(h_e - h_t)(h_e - h_r)}{\lambda d}\right)$ as introduced previously. Furthermore, although the break point $d_{break} = \frac{4 h_t h_r}{\lambda}$ has been defined based on the antenna heights and the signal wavelength, the accuracy of the path loss model above could vary around this point depending on the sea status.

Acknowledgements

References

[1] INOUE, T., AKIYAMA, T. Propagation characteristics on line-of-sight over-sea paths in Japan. *IEEE Transactions on Antennas and Propagation*, 1974, vol. AP-22, no. 4, p. 557 - 565.

[2] HITNEY, H. V., HITNEY, L. R. Frequency diversity effects of evaporation duct propagation. *IEEE Transactions on Antennas and Propagation*, 1990, vol. 38, no. 10, p. 1694 - 1700.

[3] HEEMSKERK, H. J. M., BOEKEMA, R. B. The influence of evaporation duct on the propagation of electromagnetic waves low above the sea surface at 3-94 GHz. In *Proceedings of the Eighth International Conference on Antennas and Propagation*. Edinburgh (UK), 1993, p. 348 - 351.

[4] GUNASHEKAR, S. D., WARRINGTON, E. M., SIDDLE, D. R., VALTR, P. Signal strength variations at 2 GHz for three sea paths in the British Channel Islands: Detailed discussion and propagation modeling. *Radio Science*, 2007, vol. 42, p. 1 - 13.

[5] HITNEY, H. V., RICHTER, J. H., PAPPERT, R. A., ANDERSON, K. D., BAUMGARTNER, G. B. Tropospheric radio propagation assessment. *Proceedings of the IEEE*, 1985, vol. 73, no. 2, p. 265 - 283.

[6] MALIATSOS, K., CONSTANTINOU, P., DALLAS, P., IKONOMOU, M. Measuring and modeling the wideband mobile channel for above the sea propagation paths. In *Proceedings of the 2006 First European Conference on Antennas and Propagation*. Nice (France), 2006.

[7] YANG, K., ROSTE, T., BEKKADAL, F., HUSBY, K., TRANDEM, O. Long-distance propagation measurements of mobile radio channel over sea at 2 GHz. In *Proceedings of the 2011 IEEE Vehicular Technology Conference*. San Francisco (USA), 2011.

[8] LEI, Q., RICE, M. Multipath channel model for over-water aeronautical telemetry. *IEEE Transactions on Aerospace and Electronic Systems*, 2009, vol. 45, no. 2, p. 735 - 742.

[9] MENG, Y. S., LEE, Y. H. Measurements and characterizations of air-to-ground channel over sea surface at C-band with low airborne altitudes. *IEEE Transactions on Vehicular Technology*, 2011, vol. 60, no. 4, p. 1943 - 1948.

[10] JOE, J., HAZRA, S. K., TOH, S. H., TAN, W. M., SHANKAR, J., HOANG, V. D., FUJISE, M. Path loss measurements in sea port for WiMAX. In *Proceedings of the 2007 IEEE Wireless Communications and Networking Conference*. Kowloon, 2007, p. 1871 - 1876.

[11] DONG, F., CHAN, C. W., LEE, Y. H. Channel modeling in maritime environment for USV. In *Defence Technology Asia 2011*. Singapore, 2011.

[12] LEE, Y. H., MENG, Y. S. Empirical modeling of ducting effects on a mobile microwave link over a sea surface. *Radioengineering*, 2012, vol. 21, no. 4, p. 1054 - 1059.

[13] ITU-R P.1546-4. *Method for Point-To-Area Predictions for Terrestrial Services in the Frequency Range 30 MHz to 3000 MHz*. Geneva (Switzerland): International Telecommunication Union, 2009.

[14] TETI, Jr. J. G. Wide-band airborne radar operating considerations for low altitude surveillance in the presence of specular multipath. *IEEE Transactions on Antennas and Propagation*, 2000, vol. 48, no. 2, p. 176 - 191.

[15] ITU-R P.453-10. *The Radio Refractive Index: Its Formula and Refractivity Data*. Geneva (Switzerland): International Telecommunication Union, 2012.

[16] LEE, Y. H., DONG, F., MENG, Y. S. Stand-off distances for non-line-of-sight maritime mobile applications in 5 GHz band. *Progress in Electromagnetics Research B*, 2013, vol. 54, p. 321 - 336.

[17] PARSONS, J. D. *The Mobile Radio Propagation Channel*. 2nd ed. Chichester (UK): Wiley, 2000.

[18] TIMMINS, I. J., O'YOUNG, S. Marine communications channel modeling using the finite-difference time domain method. *IEEE Transactions on Vehicular Technology*, 2009, vol. 58, no. 6, p. 2626 - 2637.

[19] ZHAO, X., HUANG, S. Influence of sea surface roughness on the electromagnetic wave propagation in the duct environment. *Radioengineering*, 2010, vol. 19, no. 4, p. 601 - 605.

[20] GUNASHEKAR, S. D., SIDDLE, D. R., WARRINGTON, E. M. Transhorizon radiowave propagation due to evaporation ducting. *Resonance*, 2006, vol. 11, no. 1, p. 51 - 62.

[21] ITU-R P.452-14. *Prediction Procedure for the Evaluation of Interference between Stations on the Surface of the Earth at Frequencies above About 0.1 GHz*. Geneva (Switzerland): International Telecommunication Union, 2009.

[22] KERANS, A., KULESSA, A. S., LENSSON, E., FRENCH, G., WOODS, G. S. Implications of the evaporation duct for microwave radio path design over tropical oceans in Northern Australia. In *Proceedings of the 2002 Workshop on the Applications of Radio Science*. Leura (Australia), 2002.

[23] LEE, W. C. Y. *Mobile Communications Engineering: Theory and Applications*. 2nd ed. McGraw-Hill, 1997.

[24] PAULUS, R. A. Practical application of an evaporation duct model. *Radio Science*, 1985, vol. 20, p. 887 - 896.

[25] LEVADNYI, I., IVANOV, V., SHALYAPIN, V. Assessment of evaporation duct propagation simulation. In *Proceedings of the XXXth URSI General Assembly and Scientific Symposium*. Istanbul (Turkey), 2011.

[26] ZHAO, X. L., HUANG, J. Y., GONG, S. H. Statistical analysis of an over-the-sea experimental transhorizon communication at X-band in China. *Journal of Electromagnetic Waves and Applications*, 2008, vol. 22, no. 10, p. 1430 - 1439.

About Authors . . .

Yee Hui LEE received the B.Eng. (Hons.) and M.Eng. degrees in Electrical and Electronics Engineering from Nanyang Technological University, Singapore, in 1996 and 1998, respectively, and the Ph.D. degree from the University of York, York, U.K., in 2002. Since July 2002, she has been with the School of Electrical and Electronic Engineering, Nanyang Technological University where she is currently an Associate Professor. Concurrently, she is also appointed as Assistant Chair (Student) for the School of Electrical and Electronic Engineering. Her interest is in channel characterization, rain propagation, antenna design, electromagnetic bandgap structures, and evolutionary techniques.

Feng DONG received the B.Eng. (Hons.) degree in Electrical and Electronics Engineering from Nanyang Technological University, Singapore, in 2010, where he is currently working toward the M.Eng degree. His research interest is in wireless channel characterizations and modeling.

Yu Song MENG received the B.Eng. (Hons.) and Ph.D. degrees in Electrical and Electronic Engineering from Nanyang Technological University, Singapore, in June 2005 and February 2010, respectively. From May 2008 to June 2009, he was a Research Engineer with the School of Electrical and Electronic Engineering, Nanyang Technological University, Singapore. Since July 2009, he has been with the Agency for Science, Technology and Research (A*STAR), Singapore. He was firstly with A*STAR's Institute for Infocomm Research as a Research Fellow, and then a Scientist I. In September 2011, he was transferred to A*STAR's National Metrology Centre where he is currently a Scientist II. His research interests include electromagnetic metrology, electromagnetic measurements and standards, and radiowave propagation.